Zhan, Hanyu; Mai, Zijun; Dai, Tingyu; Zhou, Lu; Min, Jiesheng

Coastal sediment modelling (TELEMAC-2D / TOMAWAC / GAIA): scour in offshore wind farm

Coastal sediment modelling (TELEMAC-2D / TOMAWAC / GAIA): scour in offshore wind farm

Hanyu ZHAN[1], Zijun MAI[1], Tingyu DAI[1], Lu ZHOU[2], Jiesheng MIN[2]
hyzhan@yuansuan.cn, Hangzhou, China
[1]: Zhejiang Yuansuan Technology Co., Ltd., Hangzhou, China
[2]: EDF China, R&D Center, Beijing, China

Abstract **–The radial sand ridges of the southern China Yellow Sea, located in the coastal zone where the interaction between land, sea and human activities is the strongest, is well known as the largest tidal ridges in the world. To evaluate the effects of sediment transports to an offshore wind farm, a fully coupled TELEMAC(2D)-TOMAWAC-GAIA model was thus developed to analyse the associated morpho-dynamics resulting from the influence of currents and waves.**

The process of numerical simulation was divided into two parts. Firstly, a large-scale simulation using TELEMAC-2D + TOMAWAC was performed around the China Yellow Sea and the East China Sea to obtain the boundary-imposed wave spectrum suitable for the offshore area. Secondly, a local scale coupling of TELEMAC-2D + TOMAWAC + GAIA around the radial sand ridges was performed using the wave spectrum obtained from the large-scale simulation. The influence of the pile foundation on the flow conditions was simulated by providing a drag force close to each pile foundation. The fully coupled model demonstrates its ability to simulate the sediment transports and morpho-dynamics evolution of the study area.

Keywords: Sediment transports. Non-cohesive sediment. Coupled model.

I. Introduction

The South Yellow Sea's radial sand ridge is situated south of the former Yellow River Delta and north of the Yangtze River Delta, in a shallow sea area off the coast of middle Jiangsu with rich offshore wind energy resources. The sand ridge spreads over a huge area and is characterized by a unique fan shape forming the seabed and a clear asymmetrical frame between the north and the south [1] (cf. Figure 1). Due to the interaction between ocean tides, waves and the particular properties of the sediment deposited, the bed features and their displacements are very large, causing considerable trouble to offshore wind power projects.

As a new energy resource, wind power is often regarded as green and pollution-free energy. With the maturity of the basic technology, China's offshore wind power market is gradually expanding. Up to 2021, the cumulative total installed capacity of China's offshore wind power had reached 25.35 GW [2]. During the operation and maintenance of the offshore wind farm, it was found that the pile foundations were affected by important scouring issues.

This article presents a numerical study of flow and sediment transport processes in the study area, based on the 3-way coupling 2D models of TELEMAC-2D, TOMAWAC and GAIA. Firstly, the numerical model and its setup are briefly introduced. Secondly, the model calibration against tidal and wave data is presented. Finally, numerical results are summarized and discussed.

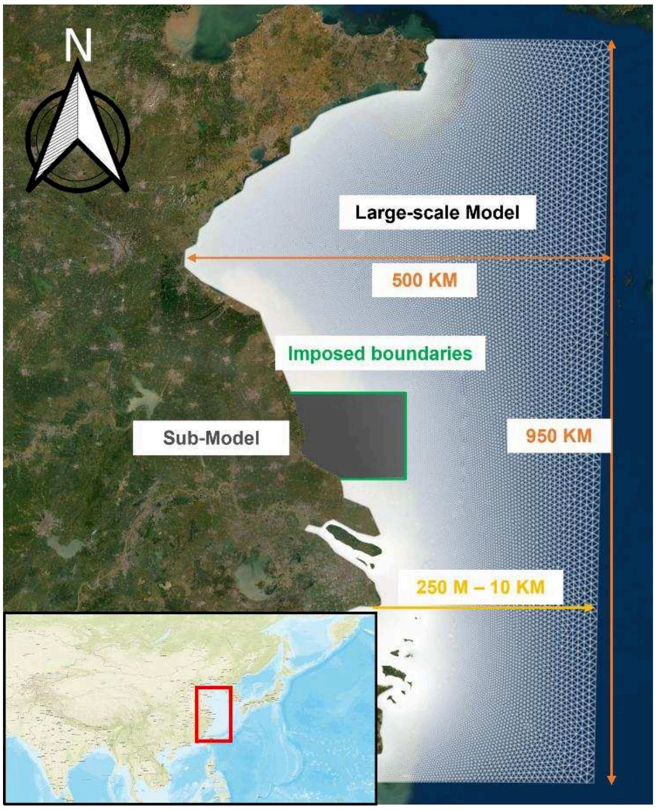

Figure 1. Study area and the nested mesh (mesh 1).

II. Numerical Model

Since the area where the wind farm is located is in offshore shoal, to reasonably consider the local wave and hydrodynamic conditions, the model is a nested model of two different scales. By considering the coupling between TELEMAC-2D and TOMAWAC in the large-scale model (cf. Figure 1), the boundary input wave spectrum of the small-scale wave model is computed. In the small-scale model (or sub-model), the Soulsby-Van Rijn formula [3] was used to compute sediment fluxes due to the combined action of waves and tides.

Hereafter, about the general modelling strategy, bathymetric and boundary conditions are briefly introduced.

A. General model

This simulation work handles a total of two meshes which are described below.

To fully account for the influence of waves in the small-scale model (sub-model), the boundaries of the waves in the sub-model are extracted from the large-scale model. The large-scale model (named Mesh 1, cf. Figure 1) contains 96,589 nodes and 189,257 elements, with a resolution varying between 250 m and 10 km, which is sufficient for wave and hydrodynamic studies. The model spans about 950 km from north to south and can reach as far as 500 km offshore and includes the sub-model at its centre.

The study area (sub-model) is also centred on the radial sand ridge in the South Yellow Sea (cf. Figure 2). The boundary of the model is about 120 km away from the coastline, and the north and south spatial span of the model is about 100 km. In this area, the transports of both bedload and suspended sands is considered for prediction of bed evolution using a three-way coupled 2D-model.

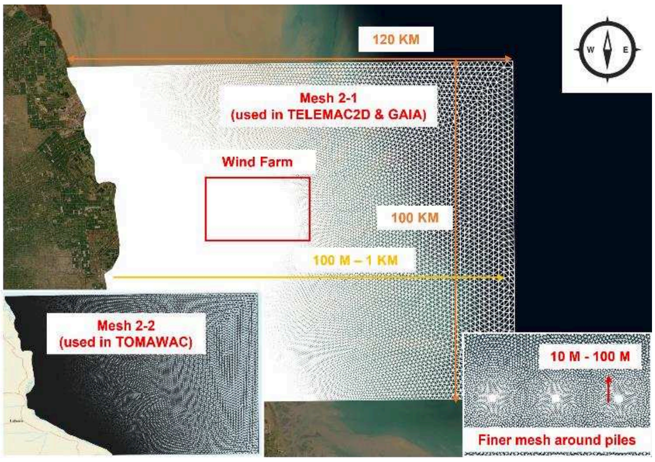

Figure 2. Mesh of sub-model used in TELEMAC-2D&GAIA (mesh 2-1) and used in TOMAWAC (mesh 2-2).

To guarantee the accuracy of the simulation over the radial ridge while being able to reduce its computation time, two meshes with different mesh resolutions are used for TELEMAC-2D and TOMAWAC modules, using the TEL2TOM feature. For TELEMAC-2D, a finer mesh (named Mesh 2-1) is used: it is progressively refined from an element size of 1 km far from the piles to an element size of 100 m close to the shore. The resolution is further adjusted to an element size of 10 m in a square domain of 100 m x 100 m around each pile. The number of elements of this mesh is 330,505 elements, and the number of nodes is 165,803. For TOMAWAC, a progressively refined mesh is adopted (named Mesh 2-2): from an element size of 1.5km far from the shore to a size of 200 m on the shore. The mesh contains 100,370 elements and 50,736 nodes.

Table I Model and corresponding mesh

Mesh Name	Mesh Properties		
	TELEMAC Module	***Mesh Size***	***Element***
Mesh 1	TELEMAC-2D/	950 km X 500 km	189 257
Mesh 2-	TELEMAC-2D/GAIA	120 km X 100 km	330 505
Mesh 2-	TOMAWAC	120 km X 100 km	100 370

B. Bathymetry

The bathymetric data in the study area was projected onto the mesh by linear interpolation using data from the General Bathymetric Chart of the Oceans (GEBCO) 2021 dataset [4]. The GEBCO dataset is a global terrain model for ocean and land, providing elevation data, in meters, on a 15 arc-second interval grid. For the large model, the seabed is gradually raised from -124 m offshore to 9 m near shore (cf. Figure 3). However, it is not the same case with the sub-model, bathymetry levels vary between -50 m and 9 m due to the radial sand ridge.

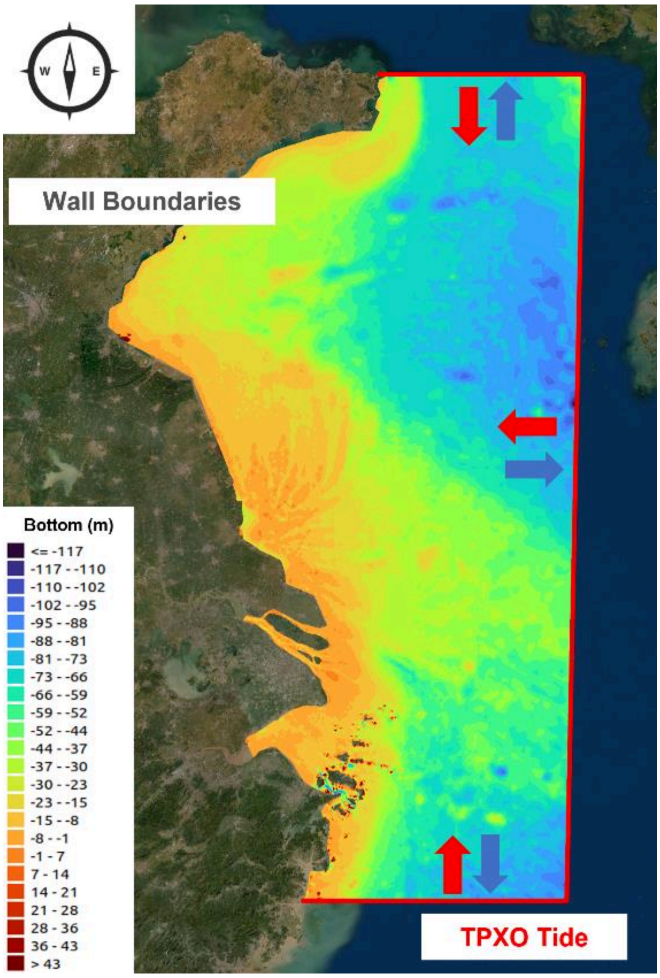

Figure 3. Bathymetry and forcing scheme of large model (TPXO Tide = Oregon State University Tidal Predicition Model).

C. Tidal boundary conditions

In both the large- and local-scale models, the liquid boundary is read from Oregon State University Tidal Prediction Model (TPXO Pacific model). TPXO is a global model of ocean tides, which best-fits, in a least-squares sense, the Laplace Tidal Equations. The methods used to compute the model are described in details by Egbert et al. 1994 [5] and further by Egbert and Erofeeva, 2002 [6].

The TELEMAC-2D model is then forced by TPXO tidal model (cf. Figs 3 and 4), providing water depth and velocities at the oceanic open boundaries to reproduce local tides in the study zone. To stabilize the hydrodynamic conditions in the early sediment simulations, a stable initial TELEMAC-2D model was computed before starting the coupling step. After testing different boundary types, both water depth (H) and velocity components (U, V) were imposed on liquid boundaries.

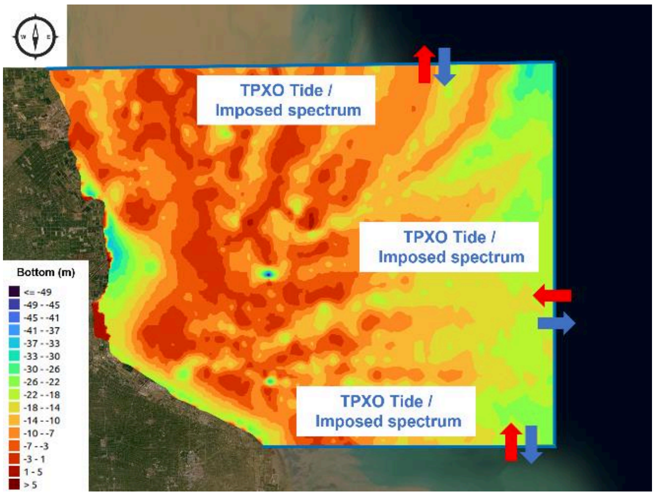

Figure 4. Bathymetry and forcing scheme of sub-model.

D. Wave boundary conditions

In the large-scale model, waves generated by the wind are considered. Dissipation mechanisms such as white-capping, depth-induced wave breaking, dissipation by bottom friction, and nonlinear wave effects between quadruplets are also modelled. Similar mechanisms are considered in the sub-model. The wave spectrum extracted from the large-scale model is imposed at the nested boundaries to better describe surges in the vicinity of the wind farm, cf. Figure 5.

As for the tides-only case, a stable initial condition of both hydrodynamics and waves is computed by considering the combined influence of tides and waves. This result is then used as initial condition for the three-way coupling model to guaranteed stability and convergence of the solution.

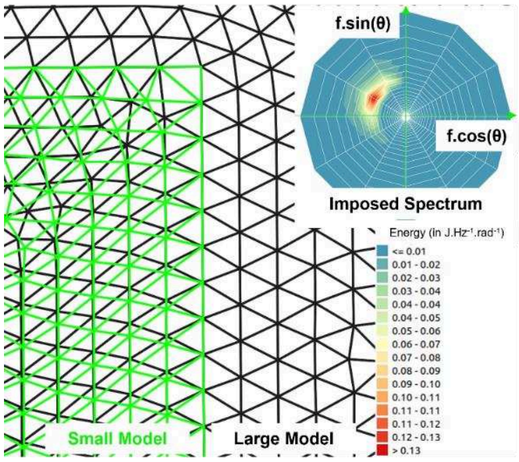

Figure 5. Imposed spectrum and boundary of TOMAWAC model.

E. Atmospheric conditions

The National Oceanic and Atmospheric Administration (NOAA/NCEP CFSv2) hourly reanalysis of wind field data is filled into the model using linear interpolation [7]. The National Centres for Environmental Prediction (NCEP) Climate Forecast System (CFS) is a fully coupled model representing the interaction between the Earth's atmosphere, oceans, land, and sea ice. CFS was developed at the Environmental Modelling Centre (EMC) at NCEP. The operational CFS has been upgraded to version 2 (CFSv2) on March 30, 2011. Wind-generated waves was computed in TOMAWAC using hourly data of 10 m high wind field. With atmospheric pressure data, the influence of wind on hydrodynamic conditions was also computed in TELEMAC-2D.

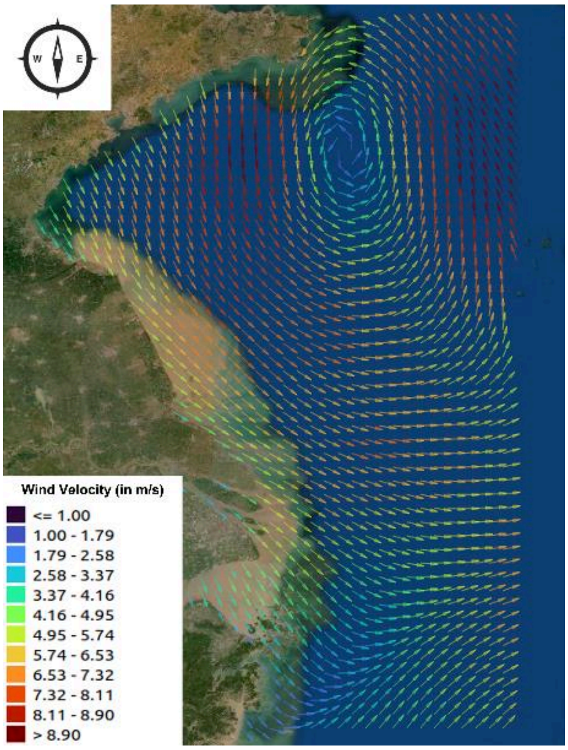

Figure 6. NOAA/NCEP CFSv2 wind data (in July 2020).

F. Bed conditions and others

Based on in-situ measurements, the sediment in the study area is mainly composed of silt with a particle size of about 0.25 mm, a porosity of 0.7, and a density of 1960 g/m^3 under wet conditions. In this work, a single layer of non-cohesive sediment was set in GAIA.

Sediment transport fluxes were computed by the Soulsby−van Rijn formula in the fully coupled model, which accounts for bedload and suspended transport processes. To account for the sediment transport direction, the slope effect is considered in the numerical simulations. Moreover, to accelerate the sediment simulation, a morphological factor equal to 5 was adopted.

To calculate the effect of wind power pile foundations on hydrodynamic conditions, drag force is computed by [8]:

$$F_D = -\frac{1}{2}\pi R^2 \rho C_D U_r |U_r|$$

Table II Acronym list of the drag force formula

Variable Name	Meaning
F_D	Drag force along the central axis of the pile foundation
R	Radius of the pile foundation
ρ	Ocean water density
C_D	Drag coefficient (1.5 was used)
U_r	Vector velocity read in TELEMAC-2D

Due to the wide range of latitude covered by the computational domain, the Coriolis force term is included in the TELEMAC-2D model. Since the seabed properties of wind farms are relatively consistent, a uniform Manning friction coefficient (0.015) is used. In addition, in order to make the computation of sediment stable, the bottom smoothing effect (BOTTOM SMOOTHINGS = 2) is considered in both TELEMAC-2D and TOMAWAC models.

III. CALIBRATION AND VALIDATION

After constructing the model and obtaining preliminary results, the authors investigated methods on how to evaluate its accuracy. This work is reported in this section.

A. Tidal model

Based on the tidal data from the National Marine Data and Information Service of China, the data of astronomical tide level was first calibrated in the hydrodynamic model.

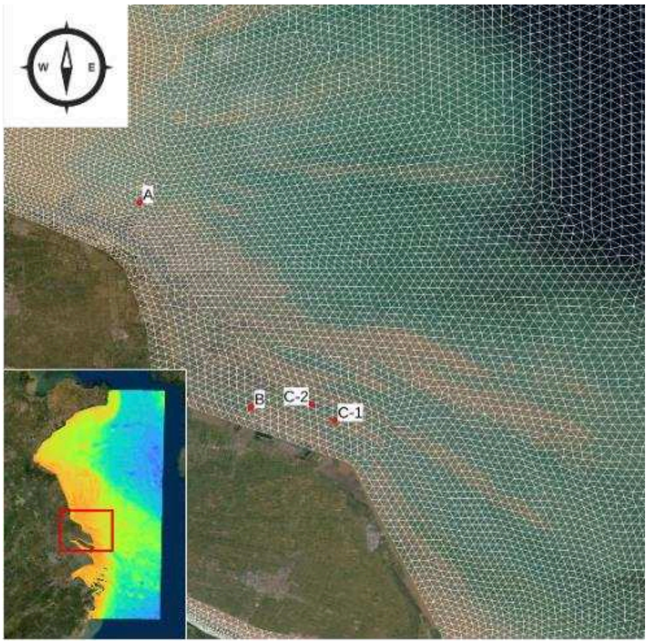

Figure 7. Positions of the stations (A/B station is for tide and C-1/C-2 station is for wave)

The water level data of local station A (cf. Figure 7) was compared with the results of the TELEMAC-2D model (data of July 2020 and data of October 2021). After the calibration of the large model, since the calibration station A is located in the area corresponding to the sub-model, the same parameters as the large-scale model, including the Coriolis force coefficient, tidal range, friction formula and coefficients, were used to compute the sub-model results. As shown in Figs 8 and 9, by comparing the 20 days' astronomical tide data, the water levels in the sub-model are well reproduced by the model with a maximum bias of about 30 cm in station A.

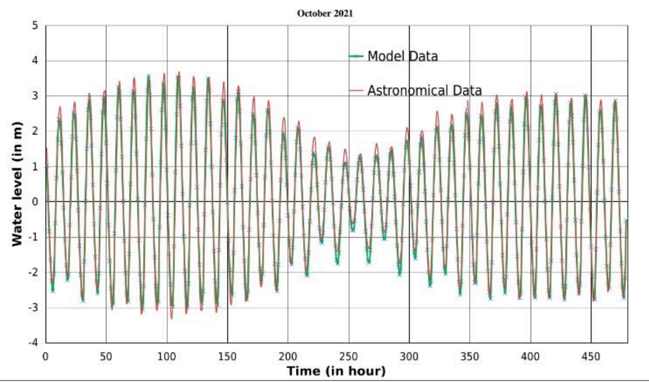

Figure 8. Comparison of water levels modelled and astronomical tide data in staton A in October 2021.

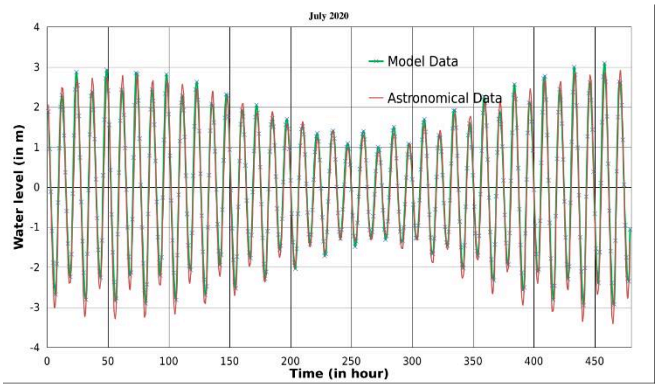

Figure 9. Comparison of water levels modelled and astronomical tide data in staton A in July 2020.

The correlation coefficient R of the comparison data is obtained using the following formula, where x and y represent the astronomical tide data and model data respectively. The correlation coefficient is 0.99 at calibration position A, cf. Figure 7.

$$R = \frac{\sum(x-\bar{x})(y-\bar{y})}{\sqrt{(\sum(x-\bar{x})^2\sum(y-\bar{y})^2)}}$$

Using the same parameters (friction coefficient, tidal range...), the results of tidal level were also obtained in station B (cf. Figure 10). The overall fitting at B station is not as good as that of A, and its correlation coefficient is about 0.94. The bias mainly exists at low tide level and neap tide. In station A, the change of water level at low tide is better calibrated, while in station B, the change of water level at high tide is better calibrated. The reason was identified to be the precision and smoothness of the bathymetry data. As the authors have not attempted to adjust the bathymetry data, this reason is speculative. This assumption will be further investigated in a future work.

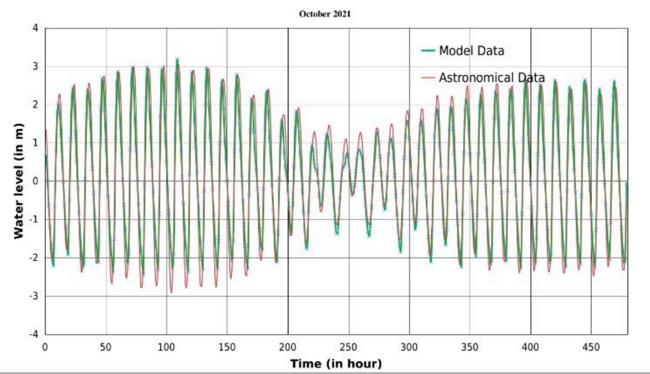

Figure 10. Comparison of water levels modelled and astronomical tide data in station B in October 2021.

B. Wave model

In the TOMAWAC model, the calibration is performed by comparing the significant wave height measured by the offshore buoy and the results. After testing different source terms and dissipation terms to calibrate the results with the measurements at buoy C-1 and C-2, it can be found that the trend and value are basically consistent, as shown in Figs 11 and 12.

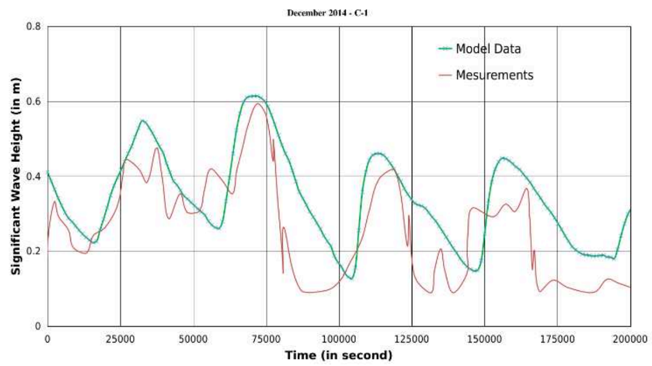

Figure 11. Comparison of significant wave height modelled and measurements in station C-1 in December 2014.

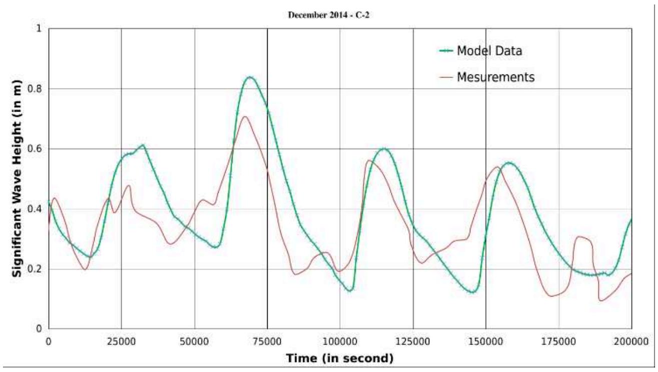

Figure 12. Comparison of significant wave height modelled and measurements in station C-2 in December 2014.

The results of calibration of significant wave height showed that the wave is well reproduced when white capping, nonlinear transfers between quadruplets, bottom friction, current dissipation, and wave breaking are considered. Therefore, in subsequent simulations , the influence of these source terms on waves is taken into account.

IV. RESULTS AND DISCUSSION

On the basis of the position of pile foundations in the wind farm, the drag force is applied by matching mesh nodes within a radius of several meters from the (x,y) coordinates of each pile foundation. To maintain the adopted Courant-Fredrichs-Lewy condition, time steps for both TELEMAC-2D and TOMAWAC sub-models are equal to 1 s and 10 s, respectively. These time-steps guarantee the stability of the solution.

In the study area, the velocity field is influenced by the drag force, with lower velocity magnitude values in the backflow direction (cf. Figure 13). Furthermore, sediment transport is strongly influenced by the combined effects of tides and waves in the dune area and the centre of the flat sandbar. In proximity of the nearshore boundary, the migration of large sediment deposit is also observed.

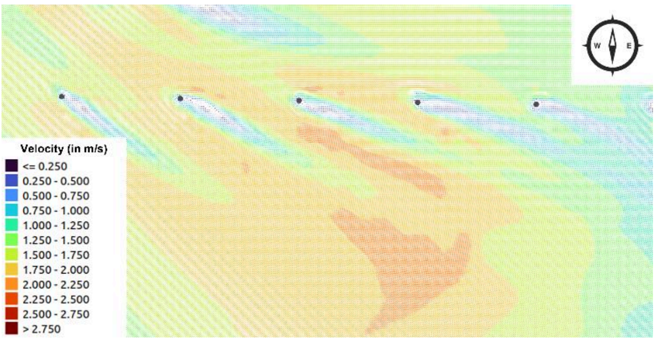

Figure 13. Velocity field near pile foundation after applying drag force

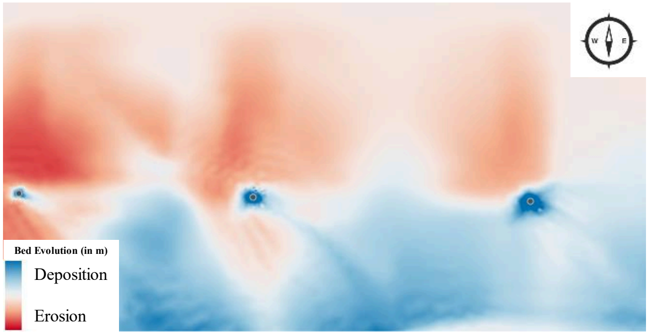

Figure 14. Erosion and deposition in wind farm around the pile foundation, the results indicate that the scour pit will be backfilled during this time.

Morpho-dynamic results show that there are some pile foundations are seriously affected by erosion and deposition. In addition, due to the drag force, in the wind farm there is an obvious tendency to strengthen the scour near some pile foundations, but there exists also scour near pile foundations that have been backfilled, as shown in Figure 14. In some areas next to the wind farm, sediment erosion or deposition is less intense than that on the other side of the wind farm, due to weaker tidal and wave conditions.

V. Conclusion

In this study, the three modules TELEMAC-2D-TOMAWAC-GAIA are coupled to to simulate sediment transport processes in an offshore wind farm area. Models of different scales are implemented in order to predict the wave conditions around an offshore windfarm.

By applying the drag force, the influence of the pile foundation on the hydrodynamic conditions and the formation of the scour pit are studied. Based on calibration for tidal and wave conditions, an attempt was made to study the evolution of scouring processes by using reanalysed wind field data. This assesses the coupling of modules TELEMAC-2D, TOMAWAC and GAIA at predicting scouring formation around offshore structures.

In future work, the model will be refined and benchmarked against actual site data to better calibrate it for predicted offshore scouring formation.

Acknowledgement

The authors would like to thank Pablo TASSI, Thierry FOUQUET, Sebastien BOURBAN from EDF R&D for their technical support on this work.

References

[1] Kang, Yanyan, Jinyan He, Bin Wang, Jun Lei, Zihe Wang, and Xianrong Ding. 2022. "Geomorphic Evolution of Radial Sand Ridges in the South Yellow Sea Observed from Satellites" Remote Sensing 14, no. 2: 287. https://doi.org/10.3390/rs14020287

[2] Statistics of China's offshore wind power installed capacity in 2021, wind energy, 2021 年中国海上风电装机统计. 风能, 2022,(08):46-49.

[3] Soulsby R. Dynamics of marine sands. H.R. Wallingford, 1997.

[4] GEBCO Compilation Group (2022) GEBCO_2022 Grid (doi:10.5285/e0f0bb80-ab44-2739-e053-6c86abc0289c)

[5] Egbert, G.D., Bennett, A.F. and Foreman, M.G.G. (1994). TOPEX/POSEIDON tides estimated using a global inverse model. Journal of Geophysical Research 99: doi: 10.1029/94JC01894. issn: 0148-0227.

[6] G. Egbert and S. Erofeeva, "Efficient inverse modeling of barotropic ocean tides," Journal of Atmospheric and Oceanic Technology, 19, 183-204, 2002.

[7] Saha, S., et al. 2011, updated daily. NCEP Climate Forecast System Version 2 (CFSv2) 6-hourly Products. Research Data Archive at the National Center for Atmospheric Research, Computational and Information Systems Laboratory. Accessed dd mmm yyyy.

[8] A. Joly, C.T. Pham, M. Andreewsky, S. Saviot, L. Fillot, Using the DRAGFO subroutine to model Tidal Energy Converters in Telemac-2D, Proceedings of the XXIInd TELEMAC-MASCARET User Conference, STFC Daresbury Laboratory, UK, 13 to 16 October 2015.